

## EFFECT OF DRY FRICTION ON BIFURCATION DIAGRAM OF FURUTA PENDULUM

VIZI Máté Benjámín<sup>1</sup>, STÉPÁN Gábor<sup>1</sup>

<sup>1</sup>*Budapest University of Technology and Economics, Faculty of Mechanical Engineering,  
Department of Applied Mechanics, Műgyetem rkp. 3, 1111 Budapest, Hungary,  
e – mail: vizi@mm.bme.hu, stepan@mm.bme.hu*

**Abstract:** Traditionally, the Furuta pendulum was used for testing advanced control strategies on a simple nonlinear and underactuated structure. In this paper, we investigate analytically and experimentally the dynamical description of the Furuta pendulum focusing on the effect of dry friction on a special bifurcation behaviour of the downward equilibrium position.

**KEYWORDS:** Furuta pendulum, dry friction, bifurcation diagram, stationary motion

### 1 Introduction

The Furuta pendulum (or rotary pendulum) is a two degree of freedom mechanical device, which consists of two arms connected to each other. The first arm rotates in the horizontal plane and its motion is usually controlled via an electrical motor. The second arm is called the pendulum, it is placed at the end of the first arm and it freely rotates in a vertical plane, which is perpendicular to the axis of the first arm. The structure of the Furuta pendulum is shown in Figure 1.

The Furuta pendulum was used to investigate advanced control strategies for balancing and swing-up of the inverted pendulum [1, 2]. While planar inverted pendula are widely used for developing control algorithms [3], the Furuta pendulum is an especially good device for this purpose because of its strongly nonlinear nature and the relatively simple and underactuated structure. The special coupling between the generalized coordinates and the gravitational force result in strongly nonlinear dynamics. The precise mechanical description capturing the full dynamics was given in [4]. The analysis of the equations of motion in the neighbourhood of certain stationary motions was presented in [5]. The bifurcation of the downward equilibrium position was investigated analytically and it was also verified by a series of measurements on an experimental rig. However, the theoretical investigations and the measurements showed a significant discrepancy, which suggested that essential dry friction was present in the experimental rig influencing the motion of the Furuta pendulum. The identification of the effect of dry friction in simple dynamical systems is an essential task in many laboratory tests and corresponding numerical simulations as shown for example in [6].

The aim of this paper is to describe and analyse the effect of the dry friction on the dynamics of Furuta pendulum focusing on the specific bifurcation behaviour.

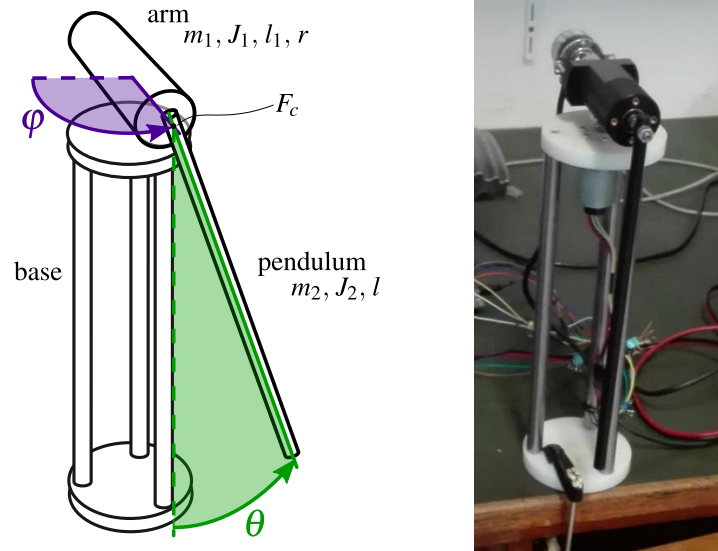


Fig. 1 Structure of the Furuta pendulum (left), experimental rig (right).

## 2 Mechanical model

All the parts of the Furuta pendulum (arm and pendulum) are assumed to be perfectly rigid. Since the Furuta pendulum is a two degree of freedom system, the two generalized coordinates are chosen to be the positions of the arm and the pendulum, which are described by the angles  $\varphi$  and  $\theta$ , respectively. The  $\theta = 0$  state means the downward position of the pendulum. The viscous damping effects are neglected, only the gravitational force and the dry friction at the pendulum pivot point are taken into account as external forces. The nonlinear equations of motion can be obtained using the Lagrangian equations of the second kind:

$$(J_a + J_p \sin^2 \theta) \ddot{\varphi} + (m_2 r l \cos \theta) \ddot{\theta} + 2J_p (\sin \theta \cos \theta) \dot{\varphi} \dot{\theta} - (m_2 r l \sin \theta) \dot{\theta}^2 = 0, \quad (1)$$

$$J_p \ddot{\theta} + (m_2 r l \cos \theta) \ddot{\varphi} - J_p (\sin \theta \cos \theta) \dot{\varphi}^2 + m_2 g l \sin \theta + F_c = 0 \quad (2)$$

where the corresponding mass moments of inertia terms are:

$$J_p = J_2 + m_2 l^2, \quad (3)$$

$$J_a = J_1 + m_1 \left(\frac{r}{2}\right)^2 + m_2 r^2, \quad (4)$$

and  $F_c$  stands for the effect of dry friction at the pivot point of the pendulum. The dry friction is considered as a set-valued function of the pendulum angular velocity  $\dot{\theta}$ :

$$F_c \begin{cases} = C, & \text{if } \dot{\theta} > 0 \\ \in (-C, C), & \text{if } \dot{\theta} = 0 \\ = -C, & \text{if } \dot{\theta} < 0 \end{cases} \quad (5)$$

Considering the assumptions described above, these equations present a special case of the ones given in [4], except the terms that includes the dry friction at the pendulum pivot point. The assumed dry friction characteristics is given in Figure 2.

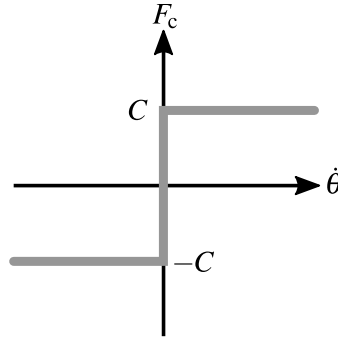


Fig. 2 Dry friction characteristics.

### 3 Equilibrium positions and stationary motions

By neglecting dry friction  $F_c = 0$  in the mechanical model and considering the solution

$$\varphi(t) = \varphi_0 + \omega_0 t, \quad \dot{\varphi}(t) = \omega_0 \quad (6)$$

of the original system (1) and (2), the equations of motion are reduced to a single equation

$$J_p \ddot{\theta} - J_p (\sin \theta \cos \theta) \omega_0^2 + m_2 g l \sin \theta = 0 \quad (7)$$

in which the  $\omega_0$  parameter is the constant angular velocity of the arm. The equilibrium positions  $\theta(t) \equiv \theta_i$  are given by the solution of

$$(m_2 g l - J_p \cos(\theta_i) \omega_0^2) \sin \theta_i = 0. \quad (8)$$

There are two or four separate equilibrium positions depending on the arm angular velocity  $\omega_0$ . The critical arm speed, where the number of equilibrium positions changes, can be calculated as

$$\omega_{\text{crit}} = \sqrt{\frac{m_2 g l}{J_p}}. \quad (9)$$

By substituting the mechanical parameters of our experimental rig (see [5]), the critical arm speed is  $\omega_{\text{crit}} \approx 7$  rad/s in our case.

The stability of all the equilibrium positions can be determined based on the linearized equations around each equilibria; the results are:

$$\theta_1 = \pi : \text{Unstable}, \quad (10)$$

$$\theta_2 = 0 : \text{Stable if } |\omega_0| < \omega_{\text{crit}}, \text{ unstable if } |\omega_0| > \omega_{\text{crit}}, \quad (11)$$

$$\theta_3 = \arccos\left(\frac{m_2 g l}{J_p \omega_0^2}\right) : \text{Stable and exists only if } |\omega_0| > \omega_{\text{crit}}, \quad (12)$$

$$\theta_4 = -\arccos\left(\frac{m_2 g l}{J_p \omega_0^2}\right) : \text{Stable and exists only if } |\omega_0| > \omega_{\text{crit}}. \quad (13)$$

The upward equilibrium position of the pendulum  $\theta_1 = \pi$  is always unstable as expected. However, the downward position  $\theta_2 = 0$  is stable for low arm speeds and loses its stability at the critical arm speed  $\omega_0 = \omega_{\text{crit}}$  and it is unstable for larger arm speeds. The emerging two other equilibrium positions  $\theta_3$  and  $\theta_4$  are stable when they exist. Therefore, the pendulum is stable in a pulled or pushed position above the critical arm speed, in other words, the pendulum points backward or forward with respect to the direction of arm rotation.

To sum up, the downward equilibrium position goes through a supercritical pitchfork bifurcation [7] with respect to the arm angular speed  $\omega_0$  as the bifurcation parameter. All the equilibrium positions and the bifurcation diagram are shown in Figure 3.

Significant dry friction is present in the experimental rig [5], so the dry friction at the pendulum pivot point is considered in the mechanical model. Examining the same solution described by Equation (6), we obtain the following equation of motion:

$$J_p \ddot{\theta} - J_p (\sin \theta \cos \theta) \omega_0^2 + m_2 g l \sin \theta + F_c = 0. \quad (14)$$

The equilibrium positions in this case are obtained as:

$$(m_2 g l - J_p \cos(\theta_i) \omega_0^2) \sin \theta_i \in (-C, C), \quad (15)$$

which can be checked numerically. Due to the dry friction, stable regions appear around all the equilibrium positions, which are also shown in Figure 3. In the case of downward position, the stable region becomes wider near to the bifurcation point  $\omega_{\text{crit}}$ . Above the critical arm speed, the stable region splits into three branches following the shape of the supercritical pitchfork bifurcation, then the width of the three stable regions shrinks as the arm speed increases further. In the case of the upward position, there is narrow stable region around the unstable equilibrium also, which means, that the dry friction can stabilize the pendulum in this position.

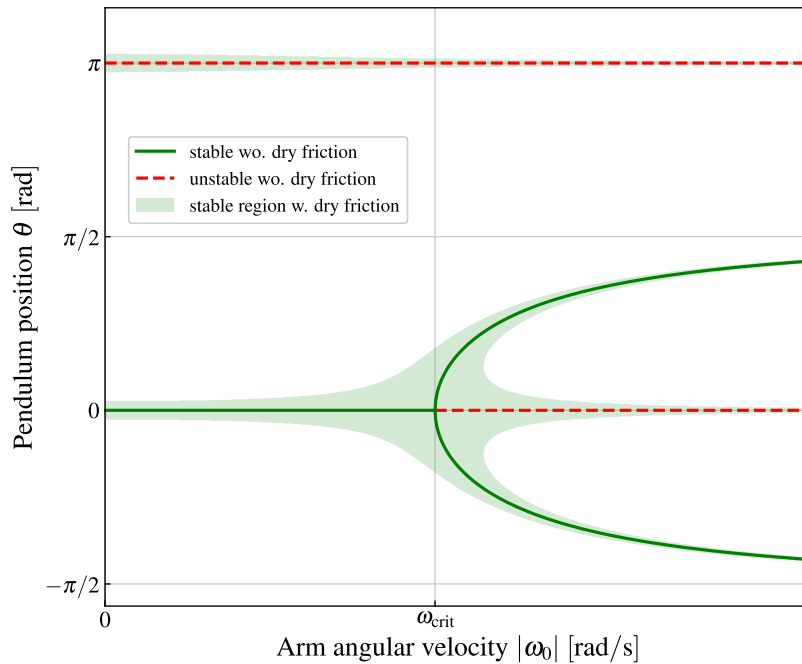


Fig. 3 Bifurcation diagram with neglecting and considering dry friction.

## 4 Measurements

Three different experiments were carried out: one for determining the dry friction parameter  $C$ , and the other two for measuring both branches of the bifurcation diagram of the downward equilibrium position.

The dry friction parameter  $C$  was measured at standstill  $\omega_0 = 0$  rad/s. The pendulum was moved up by hand, then it was let move back with slower and slower speeds, while the position where it stopped was recorded. This value practically remained the same below a certain speed, the mean value of this final position was  $\theta_{\text{mean}} = 3.17^\circ$ ; using this value we can approximate the dry friction parameter as:

$$C = m_2 g l \sin \theta_{\text{mean}} \approx 0.011 \text{ Nm.} \quad (16)$$

The stationary behaviour was also measured on the experimental rig for both the forward and backward pointing branches of the pitchfork bifurcation. An electrical DC motor was used for providing the arm angular velocity for these measurements. We started the measurement from the standing position: the input voltage of the motor was incremented by small steps, we waited some rounds to let the pendulum settle, then the pendulum position was recorded. This method was repeated until we reached the  $\omega_0 = 12$  rad/s arm speed, then we started to decrement the motor input voltage using the same steps and record the pendulum positions until the arm stopped. This way we have two sets of measurement points, one set for increasing arm speed and the other set for decreasing arm speed. The two sets of measurement points differ from each other significantly by presenting a hysteresis.

For the increasing speed measurements, the downward position of the pendulum remains stable even above the critical arm speed, so some measurement points lie on the (unstable) red dashed line in Figure 3 showing that the dry friction stabilizes the pendulum. Then the pendulum jumps to one or the other stable branches of the pitchfork bifurcation (pointing backward or forward, respectively) where the dry friction-induced stable region becomes narrow. The pendulum continues to rise as the arm speed increases.

For the decreasing speed measurements, the pendulum goes back on a different path which is near the outer edge of the dry friction-induced stable region. This difference means that there is a significant hysteresis caused by the dry friction. At the end of the measurement with zero arm speed, the final position of the pendulum is only in the vicinity of the initial vertical position and it is near the edge of the stable region caused by the effect of dry friction.

The Figures 4 and 5 show the measurements for the cases when the pendulum points backward and forward during the rotation, respectively. The measured dry friction constant was used for illustrating the true stable region of the experimental rig in these figures.

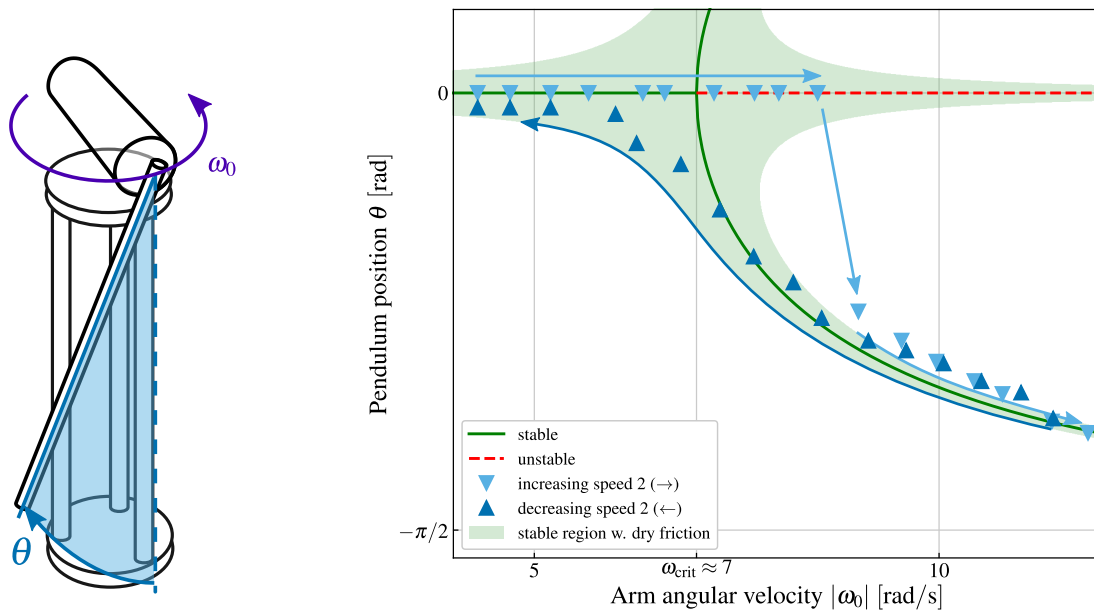


Fig. 4 Measurement of the steady motion for backward pointing pendulum.

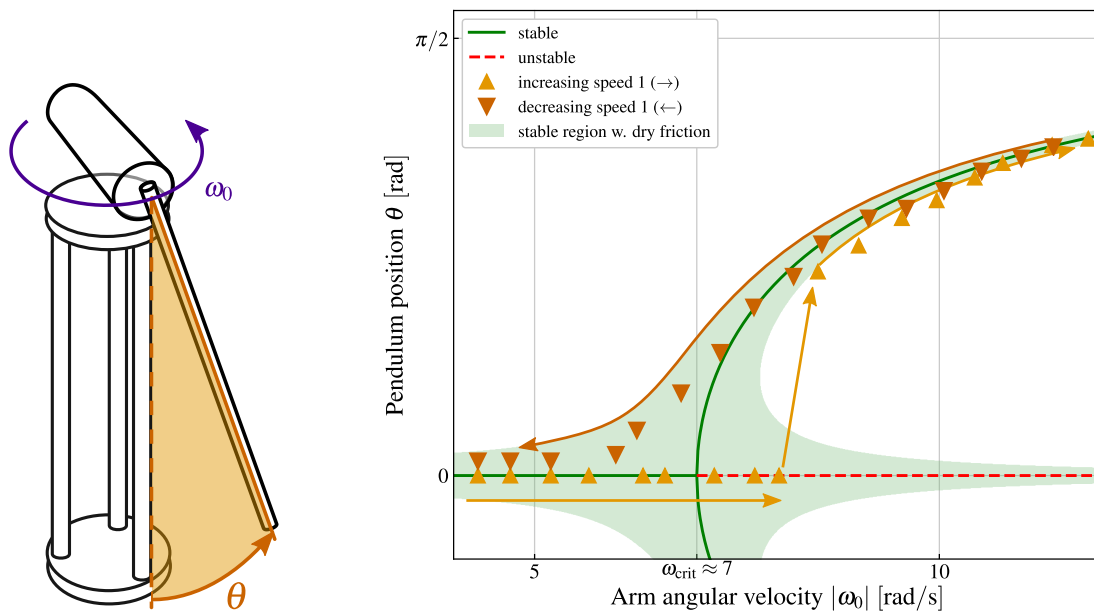


Fig. 5 Measurement of the steady motion for forward pointing pendulum.

## CONCLUSION

The bifurcation diagram containing all the theoretical results and the measurements are shown in Figure 6. The true size of the stable region is represented based on preliminary experiments. The measurements on the rotating Furuta pendulum were carried out for the downward position and they show good agreement with the theoretical calculations assuming the dry friction. During the measurements with increasing speed, the stable region was identified also around the unstable branch, when the width of stable region is too narrow, then some perturbations make the measurements jump to the neighbourhood of the stable branches, therefore, the stable region around the unstable branch is only vaguely attractive. During the

measurements with decreasing speed, significant hysteresis was detected in the dynamic behaviour, which is also caused by dry friction.

These results and observations are to be used in future work on establishing control strategy for stabilizing the upper position of the Furuta pendulum.

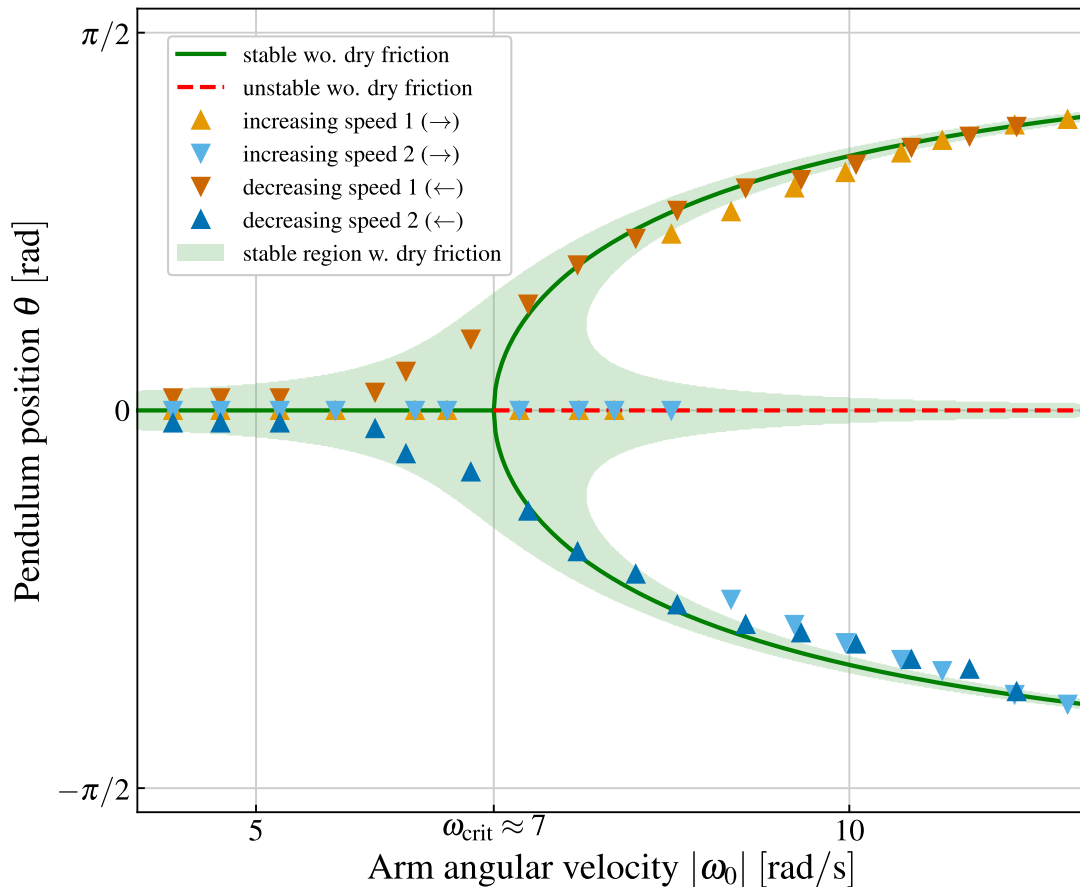


Fig. 6 Bifurcation diagram containing all the results.

## REFERENCES

- [1] K. Furuta, M. Yamakita, S. Kobayashi. Swing up control of inverted pendulum. In *Industrial Electronics, Control and Instrumentation, 1991. Proceedings. IECON'91., 1991 International Conference on, IEEE, 1991*, 2193 – 2198.
- [2] K. Furuta, M. Yamakita, S. Kobayashi. Swing-up control of inverted pendulum using pseudo-state feedback. *Proceedings of the Institution of Mechanical Engineers, Part I: Journal of Systems and Control Engineering* **1992** (206), No. 4, 263 – 269.
- [3] M. Mates, D. Nyeky, M. Honek, B. Rohal'-Ilkiv. Control of inverted pendulum laboratory system using stepper motor. *Journal of Mechanical Engineering – Strojnícky časopis* **2009** (60), No 4., 211 – 220.
- [4] B. S. Cazzolato, Z. Prime. On the dynamics of the furuta pendulum. *Journal of Control Science and Engineering* **2011**, p. 8. Article ID 528341. DOI: 10.1155/2011/528341
- [5] M. B. Vizi, G. Stepan. Experimental Bifurcation Diagram of Furuta Pendulum, Paper No. DSCC2018-9030, ASME 2018 DSCC Atlanta, Georgia, USA, Sept. 30-Okt 4., **2018**.

- [6] J. Stein, R. Chmúrny. Comparison of phenomenological methods for dry-friction simulation of an oscillatory system under random excitation. *Journal of Mechanical Engineering – Strojnícky časopis* **2012** (63), No 5 – 6, 261 – 276.
- [7] J. M. T. Thompson, H. B. Stewart. *Nonlinear dynamics and chaos*. John Wiley & Sons, **2002**.